

On the Commensurate Phase in the Second Layer of Helium on Graphite: A New Quantum Phase?

S. Nakamura, K. Matsui, T. Matsui, and Hiroshi Fukuyama*

*Department of Physics, The University of Tokyo,
7-3-1 Hongo, Bunkyo-ku, Tokyo 113-0033, Japan*

(Dated: December 6, 2024)

The second-layer phase diagrams of ^4He and ^3He adsorbed on graphite are investigated from heat-capacity measurements below 2 K at densities where He films solidify due to strong correlations and a periodic potential created by underlayers. In contrast to a recent first-principles simulation, we observed large heat-capacity anomalies in both isotopes which indicate unambiguously the existence of a distinct phase stabilized by the weak periodic potential, most likely a commensurate solid, over an extended density region between liquid and incommensurate solid phases. We propose novel states of matter including a quantum solid with *zero-point defectons* for this phase where exotic ground states such as supersolid or gapless quantum spin-liquid are expected.

Helium (He) monolayers adsorbed on an atomically flat and strongly attractive graphite surface provide unique arenas to investigate low-dimensional effects and resultant novel quantum phases. One important example is the gapless quantum spin-liquid state found in the commensurate phase in the second layer, hereafter the C2 phase, of ^3He with nuclear spin $1/2$ [1–3]. This is a two dimensional (2D) fermionic quantum solid with a triangular lattice structure. The commensurability here is with respect to the triangular lattice of the compressed first layer. Since several promising electronic counterparts have been found during the last decade, this new magnetic state is now attracting much attention [4]. Further novel strong-correlation effects are discussed in the supposed hole-doped C2 phase of ^3He [5]. In the second layer of ^4He , a 2D bosonic system, two previous torsional oscillator experiments [6, 7] observed a reentrant superfluid response as a function of density below 400 mK. The supersolidity in the C2 phase, in which both lattice translational and gauge symmetries are spontaneously broken [8, 9], is one of exciting possibilities to explain the observations.

Compared to the low temperature properties, details of the phase diagram around the C2 phase particularly structural information are quite limited. Neutron scattering experiments [10] failed to detect Bragg peaks from the C2 phase. Heat capacity data for ^4He [11] and ^3He [12] films show rounded peaks at 1.4 and 0.9 K, respectively, at densities between the liquid (L2) and incommensurate solid (IC2) phases. The peaks are assigned to melting transitions of the C2 phases. Since they are found at similar density ratios around $4/7$ between the first and second layers, the phase is called the “ $4/7$ phase” or more specifically the $\sqrt{7} \times \sqrt{7}$ phase (see the inset of Fig. 1(c)). Such structural assignment has been confirmed by several computational simulations [13–15]. In addition, the $4/7$ phase is also found in ^3He monolayers adsorbed on graphite preplated with monolayer of ^4He ($^3\text{He}/^4\text{He}/\text{gr}$) [2, 16, 17] or a bilayer of HD molecules ($^3\text{He}/\text{HD}/\text{HD}/\text{gr}$) [2, 18, 19].

The previous belief on the $4/7$ phase has recently been seriously thrown into doubt by the path integral Monte Carlo (PIMC) calculation for ^4He by Corboz *et al.* [20]. They claimed that the C2 phase is not stabilized against the L2 and IC2 phases if zero-point vibrations of the first layer atoms are explicitly taken into account. They also found that the $7/12$ phase (not the $4/7$ phase) can be stabilized only when (i) the first layer atoms are held fixed or (ii) they assume a 10% deeper He-graphite potential than widely accepted one [21] and a rather high first-layer density ($= 12.7 \text{ nm}^{-2}$) compared to the second-layer promotion density ($= 11.7 \text{ nm}^{-2}$) calculated by themselves. The absence of the C2 phase was also reported in recent calculations on graphene which has 14% shallower potential than graphite [22]. The apparent discrepancy between the previous understanding and the recent PIMC calculation [20] raised serious questions: Is the C2 phase stabilized artificially, for example, by finite size effects due to the microcrystalline (platelet) structure of exfoliated graphite substrate used in the previous experiments? Are the heat capacity peaks observed in ^4He and ^3He the same phenomenon and related to melting transition?

In this Letter, we report results of new heat capacity measurements of the second layers of pure ^4He and ^3He films in a temperature range between 0.1 and 1.9 K using a ZYX exfoliated graphite substrate. ZYX is known to have ten times larger platelet size (100–300 nm) [23] than Grafoil, a substrate used in all previous works. We obtained unambiguous thermodynamic evidences for the existence of a distinct phase (C2 phase) between the L2 and IC2 phases and that the phase exists in an extended density window. Novel possibilities such as quantum solid with zero-point defectons are suggested for this phase, which provides a key basis for the emergence of the currently discussed exotic ground-states.

The experimental setup used here has been described in detail elsewhere [24]. The heat capacity was measured by the heat pulse method with variable constant heat flows. In the following we show only the heat capac-

ity of adsorbed He films after subtracting the addendum (empty cell) and the desorption contribution (see below). The surface area of the ZYX substrate is $30.5 \pm 0.2 \text{ m}^2$. The vapor pressure of sample is monitored with an *in situ* capacitive strain gauge.

The much larger platelet size of our ZYX than Grafoil is well demonstrated by observing a two times higher specific heat peak at the order-disorder transition ($T = 2.9 \text{ K}$) for the $\sqrt{3} \times \sqrt{3}$ commensurate phase of ^4He adsorbed directly on graphite (see Figs. 1 and 2 of Ref. 25). The critical region is also wider in ZYX being consistent with the finite size scaling. Here the commensurability of this phase is with respect to the graphite honeycomb lattice. Despite the larger platelet size, ten times smaller specific surface area ($2 \text{ m}^2/\text{g}$) of ZYX causes much larger desorption heat-capacity contribution. This prevents us from analyzing experimental data with reasonable accuracies at temperatures higher than 1.8–1.9 and 1.3–1.4 K for ^4He and ^3He , respectively.

Let us first show T -dependencies of measured heat capacities (C) of ^4He films at densities of $17.50 \leq \rho \leq 19.73 \text{ nm}^{-2}$ in Fig. 1(a) and $19.73 \leq \rho \leq 21.01 \text{ nm}^{-2}$ in Fig. 1(b). Here ρ is the total areal density. Since the first-layer has a much higher density or Debye temperature than the second layer, its heat capacity contribution is less than 3% in the T -range we studied. At the lowest ρ (17.50 nm^{-2}) the system is a uniform 2D liquid. At high T , this phase is characterized by a nearly constant C slightly less than the $N_2 k_B$ expected for an ideal 2D gas as well as a broad maximum near 0.9 K below which C rapidly falls down [11, 26]. Here N_2 is the number of He atoms in the second layer estimated by assuming a constant first-layer density (ρ_1) of 12.2 nm^{-2} . This ρ_1 value is evaluated from the second-layer promotion density ($= 11.8 \pm 0.3 \text{ nm}^{-2}$) [25] and the subsequent compression of the first layer by 3% [10]. As ρ increases above 18.70 nm^{-2} , a new C anomaly starts to develop near $T = 1.4 \text{ K}$ whereas the liquid component gradually decreases. The two features coexist until 19.47 nm^{-2} . Above 19.64 nm^{-2} the liquid component completely disappears leaving only the rounded peak at 1.4 K which corresponds to the C2 peak observed by Greywall [11] using Grafoil substrate. As we further increase ρ , the heat-capacity peak height (C_{peak}) becomes largest at 19.73 nm^{-2} ($\equiv \rho_{C2}$) and then turns to decrease. In Fig. 1(c) the specific heat data at ρ_{C2} obtained with ZYX and Grafoil are compared. They look similar each other except that the ZYX data give a slightly larger specific heat around and above T_{peak} by about 13%. Above 20.44 nm^{-2} a new peak appears near 0.8 K. With increasing ρ , the peak grows rapidly in height and temperature up to 1.2 K coexisting with the C2 anomaly which diminishes gradually keeping T_{peak} fixed. The two features apparently coexist at least until 20.80 nm^{-2} . This last peak is associated with melting transition of the IC2 solid [11, 26]. The third layer promotion occurs at den-

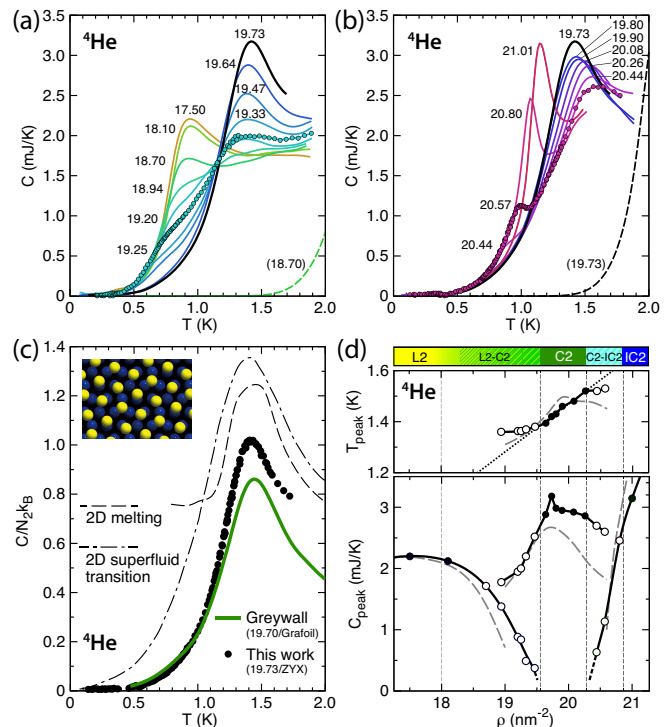


FIG. 1. (a) (b) Heat capacities of the second layer of ^4He on ZYX graphite. The numbers are total densities in nm^{-2} . For clarity actual data points are plotted only for 19.25 and 20.57 nm^{-2} . The dashed lines are desorption contributions which have already been subtracted from the raw data. (c) Specific heat of the C2 phase obtained with ZYX (filled circles: this work) and Grafoil (solid line: Ref. 11) substrates. Also shown are calculated specific heats for 2D melting (dashed line: Ref. 27) and superfluid transition (dash-dotted line: Ref. 28). They are normalized by T_{peak} . The inset shows a schematic top view of the $4/7$ phase proposed in Ref. 15. (d) Density variations of C_{peak} (lower panel) and T_{peak} (upper panel). The filled symbols are for the pure L2, C2 and IC2 phases and open ones for the coexistence regions. The dashed lines are the data of Ref. 11 adjusted to our surface area. The dotted line is the T_c vs. ρ_s relation in the Kosterlitz-Thouless theory (see text).

sities above 21 nm^{-2} [11] after the major compression of the second layer.

In Fig. 1(d) we plot density variations of C_{peak} and T_{peak} as well as those of Greywall [11] (dashed lines) who used Grafoil substrate. The phase diagram determined in this work is also shown on the top. Unambiguously, there exists a distinct C2 phase over an extended density region from 19.6 to 20.3 nm^{-2} where we observed only the C2 anomaly (closed circles). The C2 phase is not an experimental artifact caused by finite size effects of substrate since the specific heat anomaly is even enhanced slightly with increasing the platelet size by an order of magnitude. Within this C2 region, T_{peak} increases by 10% almost linearly with increasing ρ . The C2 phase is well separated from the L2 and IC2 phases by L2-C2 ($18 < \rho <$

19.6 nm⁻²) and C2-IC2 (20.3 < ρ < 20.9 nm⁻²) coexistence regions where we observed the double anomaly feature (open circles). This feature is also seen in Greywall's data at 19.00 and 20.30 nm⁻² (see Fig. 3 of Ref. 11). However, thanks to finer ρ - and T -grids and the better substrate quality, we could obtain much more informative data. For example, the L2-C2 and C2-IC2 coexistence regions share a remarkable feature as follows. When ρ approaches ρ_{C2} , the L2 and IC2 anomalies destruct preferentially from higher- T envelopes keeping common low- T envelopes, while the C2 anomaly grows without changing its T_{peak} so much. This strongly suggests the commensurate nature of the C2 phase and non-macroscopic two phase coexistence perhaps with domain wall structures, since only the more compressible L2 and IC2 phases seem to be changing their excitation spectra.

Next we show heat capacity data of the second layer of ³He films at densities of 17.50 ≤ ρ ≤ 19.00 nm⁻² in Fig. 2(a) and 19.00 ≤ ρ ≤ 20.40 nm⁻² in Fig. 2(b). The density evolution is qualitatively similar to that in ⁴He. We observed again a clear C2 peak which becomes maximum at $\rho_{C2} = 19.1 \pm 0.1$ nm⁻² and $T_{\text{peak}} = 1.0$ –1.1 K. This peak is very similar to that observed by Van Sciver and Vilches using Grafoil [12] as compared

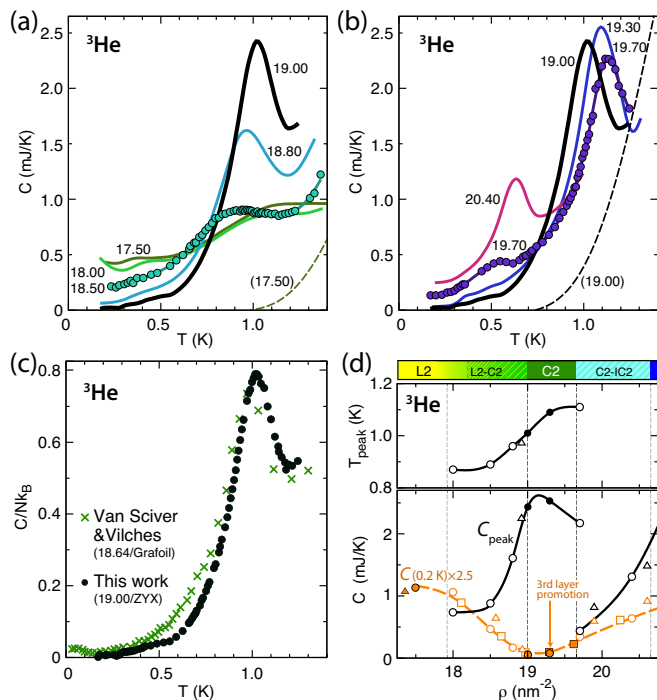


FIG. 2. (a) (b) Heat capacities of the second layer of ³He on ZYX. (c) Specific heat of the C2 phase obtained with ZYX (filled circles: this work) and Grafoil (crosses: Ref. 12). (d) Density variations of C_{peak} (lower panel) and T_{peak} (upper panel). The dashed line is a heat capacity isotherm at $T = 0.2$ K. The triangles (Refs. 12, 29) and squares (Ref. 30) are the data with Grafoil adjusted to our surface area and density scale (see text). Other details are the same as Fig. 1.

in Fig. 2(c), indicating almost no size effects. Here we estimated N_2 assuming $\rho_1 = 11.6$ nm⁻². This ρ_1 value is evaluated from the second-layer promotion density ($= 11.2 \pm 0.2$ nm⁻²) [26] and the subsequent first-layer compression of 4% [10]. We should also point out that their data have slightly larger specific heats at low- T due to a small amount of remnant L2 phase (see below). In Fig. 2(d) we plot density variations of C_{peak} and T_{peak} for ³He as well as a proposed phase diagram at $T = 0$. The determination of each phase boundary is somewhat ambiguous compared to ⁴He. This is partly because the density grid of measurement is not fine enough here, and partly because the double peak feature in the coexistence regions is hardly observable due to weakly T -dependent large C contributions from Fermi liquids in the second and third layers. These contributions are represented by the heat capacity isotherm at $T = 0.2$ K plotted in Fig. 2(d). The previous workers' data with Grafoil seem to be consistent with our phase diagram if their density scales are multiplied by 1.015 for Refs. 12, 29 and 1.04 for Ref. 30. The third layer promotion in ³He occurs at a relatively low density (≈ 19.3 nm⁻²) before the C2-IC2 coexistence starts [26, 30].

The low- T specific heat of the ³He-C2 phase is well fitted to $C/N_2k_B = \alpha T^2 + \beta \exp(-E_g/T)$ below 0.7 K, where $\alpha = 0.14$ K⁻², $\beta = 4.1 \times 10^2$ and $E_g = 6.2$ K, as shown in Fig. 3(a). The $C \propto T^2$ behavior is expected from 2D phonon excitations. The coefficient α is only $9 \pm 3\%$ smaller than that estimated from the known relation between α and T_{peak} for the IC solid ³He in the first layer [12] suggesting the 2D solid nature. Unfortunately, we could not conclude if the ⁴He data follow the $C \propto T^2$ behavior or not mainly due to limited accuracies of the data below 0.6 K.

The overall T -dependencies of the anomalies look reasonably similar between the two isotopes as shown in Fig. 3(b), suggesting a common phenomenon behind, though the ³He anomaly is slightly narrower. Also considering the apparent scalability of C_{peak}/N_2k_B with

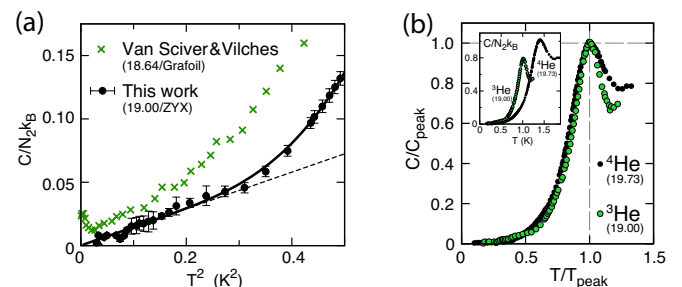


FIG. 3. (a) Low- T specific heat of the C2 phase of ³He plotted as a functions of T^2 . The crosses are the data in the L2-C2 region from Ref. 12 where a liquid-like nearly T -independent contribution coexists with a T^2 contribution. (b) Comparisons between the ⁴He- and ³He-C2 anomalies on ZYX.

T_{peak} (inset of Fig. 3(b) [31]) and the similarity of the phase diagrams, it is likely associated with the 2D melting transition of the Kosterlitz-Thouless-Halperin-Nelson-Young (KTHNY) type [32]. In this case, an intrinsically rounded specific-heat anomaly appears at a somewhat higher T than the critical temperature (T_c) due to unbinding of topological defects such as dislocations or disclinations. Eventually, the experimental C2 anomalies fairly resemble to a calculated specific heat based on the KTHNY theory [27] as seen in Fig. 1(c). The absence of size effects on C_{peak} and the gap-like behavior of low- T envelope of anomaly are consistent with this picture.

To our knowledge, there are no other candidates for the ^4He - and ^3He -C2 phases than commensurate solids in a broad sense which are barely stabilized by a weak periodic potential of underlayers with a oscillation amplitude of about 0.5 K [26]. This is also supported by the fact that experimental density ratios between the first and second layers are identical within experimental errors for both isotopes, i.e., 0.62 ± 0.05 (^4He) and 0.65 ± 0.03 (^3He), although they are larger than $4/7 = 0.571$. Curiously enough, the C2 phases are stabilized in extended density regions as wide as $w \equiv \Delta\rho_{\text{C2}}/\rho_{\text{C2}} \approx 0.10$ and 0.04 for ^4He and ^3He , respectively, regardless of the platelet size. Within this region T_{peak} increases linearly with ρ , i.e., the C2 phase is compressed, while C_{peak} has a maximum near the lowest density bound.

How can we explain the compressibility of commensurate solid? There seem to be two possibilities which explain the compressibility of commensurate solid [33]. (I) The C2 phase is a commensurate solid which can accommodate large amounts of interstitial particles (and perhaps some vacancies as well). Those interstitials should be *zero-point defectons* which exchange quantum mechanically with atoms occupying commensurate sites. This gives rise to “fluidity” to crystal even at $T = 0$. The zero-point defectons in quantum solids were predicted long ago by Andreev [8, 34] but have never been found experimentally. (II) A *quantum liquid crystal* state, where translational or rotational symmetries are partially broken, may also be possible. In both cases, supersolidity will be expected for ^4He at sufficiently low T . In connection with this, we should point out that the T_{peak} vs. ρ_2 data for ^4He are in surprisingly close proximity to the T_c vs. ρ_s relation in the Kosterlitz-Thouless theory [35] for 2D superfluidity of the whole second layer (the dotted line in Fig. 1(d)) but not for ^3He . Here ρ_2 is the second-layer density and ρ_s is the superfluid density.

In summary, we determined the phase diagrams of the second layer of ^4He and ^3He on graphite near solidification from heat capacity measurements below 2 K. We obtained experimental evidences for the existence of a distinct phase (C2 phase) at densities between the liquid and incommensurate solid phases in both isotopes unlike the recent calculation [20]. The most probable assign-

ment for the C2 phase is a commensurate quantum solid with zero-point defectons, a new class of matter. The ground states of bosonic (^4He) and fermionic (^3He) C2 phases should be of great interest to investigate further.

We thank Tony Leggett for illuminating discussions and suggestions. This work was financially supported by Grant-in-Aid for Scientific Research on Priority Areas (Grant No. 17071002) from MEXT, Japan and Scientific Research (A) (Grant No. 22244042) from JSPS. S. N. acknowledges support from the Fuuju-kai Fellowship.

* hiroshi@phys.s.u-tokyo.ac.jp

- [1] K. Ishida, M. Morishita, K. Yawata, and H. Fukuyama, Phys. Rev. Lett. **79**, 3451 (1997); H. Fukuyama and M. Morishita, Physica B **280**, 104 (2000).
- [2] R. Masutomi, Y. Karaki, and H. Ishimoto, Phys. Rev. Lett. **92**, 025301 (2004).
- [3] H. Fukuyama, J. Phys. Soc. Jpn. **77**, 111013 (2008); Note that the “C2 phase” defined in this review is another commensurate solid hypothesized to exist at a much higher density than the C2 phase in this Letter. The existence has recently been renounced by a new careful heat-capacity measurement by D. Sato *et al.* (to appear).
- [4] L. Balents, Nature **464**, 199 (2010) and references therein.
- [5] Y. Fuseya and M. Ogata, J. Phys. Soc. Jpn. **78**, 013601 (2009); S. Watanabe and M. Imada, J. Phys. Soc. Jpn. **78**, 033603 (2009).
- [6] P. A. Crowell and J. D. Reppy, Phys. Rev. B **53**, 2701 (1996).
- [7] Y. Shibayama, H. Fukuyama, and K. Shirahama, J. Phys.: Conf. Ser. **150**, 032096 (2009).
- [8] A. F. Andreev and I. M. Lifshitz, Sov. Phys. JETP **29**, 1107 (1969).
- [9] H. Matsuda and T. Tsuneto, Prog. Theor. Phys. Suppl. **46**, 411 (1970).
- [10] H. J. Lauter, H. P. Schildberg, H. Godfrin, H. Wiechert, and R. Haensel, Can. J. Phys. **65**, 1435 (1987); M. Roger, C. Bäuerle, H. Godfrin, L. Pricoupenko, and J. Treiner, J. Low Temp. Phys. **112**, 451 (1998).
- [11] D. S. Greywall, Phys. Rev. B **47**, 309 (1993).
- [12] S. W. Van Sciver and O. E. Vilches, Phys. Rev. B **18**, 285 (1978).
- [13] F. F. Abraham, J. Q. Broughton, P. W. Leung, and V. Elser, Europhys. Lett. **12**, 107 (1990).
- [14] M. Pierce and E. Manousakis, Phys. Rev. B **59**, 3802 (1999).
- [15] T. Takagi, J. Phys.: Conf. Ser. **150**, 032102 (2009).
- [16] E. Collin, S. Triqueneaux, R. Harakaly, M. Roger, C. Bäuerle, Y. M. Bunkov, and H. Godfrin, Phys. Rev. Lett. **86**, 2447 (2001).
- [17] D. Sato, D. Tsuji, S. Takayoshi, K. Obata, T. Matsui, and H. Fukuyama, J. Low Temp. Phys. **158**, 201 (2010).
- [18] M. Siqueira, C. P. Lusher, B. P. Cowan, and J. Saunders, Phys. Rev. Lett. **71**, 1407 (1993); A. Casey, H. Patel, J. Nyéki, B. Cowan, and J. Saunders, J. Low Temp. Phys. **113**, 265 (1998).
- [19] H. Ikegami, R. Masutomi, K. Obara, and H. Ishimoto,

- Phys. Rev. Lett. **85**, 5146 (2000).
- [20] P. Corboz, M. Boninsegni, L. Pollet, and M. Troyer, Phys. Rev. B **78**, 245414 (2008).
- [21] W. E. Carlos and M. W. Cole, Surf. Sci. **91**, 339 (1980).
- [22] M. C. Gordillo and J. Boronat, Phys. Rev. B **85**, 195457 (2012); Y. Kwon and D. M. Ceperley, Phys. Rev. B **85**, 224501 (2012); J. Hap-pacher, P. Corboz, M. Boninsegni, and L. Pollet, Phys. Rev. B **87**, 094514 (2013).
- [23] Y. Niimi, T. Matsui, H. Kambara, K. Tagami, M. Tsukada, and H. Fukuyama, Phys. Rev. B **73**, 085421 (2006); R. Bir-geneau, P. Heiney, and J. Pelz, Physica B+C **109–110, Part 3**, 1785 (1982), 16th International Conference on Low Temperature Physics.
- [24] S. Nakamura, K. Matsui, T. Matsui, and H. Fukuyama, J. Phys.: Conf. Ser. **400**, 032061 (2012).
- [25] S. Nakamura, K. Matsui, T. Matsui, and H. Fukuyama, J. Low Temp. Phys. **171**, 711 (2013); The T -dependent correction applied to the raw heat-capacity data above 2.2 K in this reference is totally unnecessary in the present experiment.
- [26] S. Nakamura, K. Matsui, T. Matsui, and H. Fukuyama, to appear.
- [27] K. Wierschem and E. Manousakis, Phys. Rev. B **83**, 214108 (2011).
- [28] D. M. Ceperley and E. L. Pollock, Phys. Rev. B **39**, 2084 (1989).
- [29] S. W. Van Sciver, Phys. Rev. B **18**, 277 (1978).
- [30] D. S. Greywall, Phys. Rev. B **41**, 1842 (1990); Note that the surface area in this reference was corrected by -2.5% in D. S. Greywall and P. A. Busch, Phys. Rev. Lett. **65**, 64 (1990).
- [31] We should, however, keep in mind that the C_{peak} might not be the maximum one if we failed to pinpoint the true ρ_{C2} in ^3He .
- [32] It is less plausible that intrinsically much sharper specific-heat anomalies, for example, due to order-disorder transitions are thermally smeared out by desorption because the ^3He -C2 peak, for which the desorption contribution is larger, is sharper than the ^4He one. Instead, thermally-activated interlayer mixing may play some roles on the smearing or on the transition nature.
- [33] One may consider that the apparent compression of the C2 phase is a result of the simultaneous compression of the first and second solid layers with increasing ρ keeping the density ratio fixed. Eventually, the neutron scattering experiments of Ref. 10 revealed 2% increase of ρ_1 at corresponding densities both for ^4He and ^3He . However, this increase cannot explain $w = 0.10$ for ^4He quantitatively nor the ρ -dependence of C_{peak} . Moreover, in $^3\text{He}/\text{HD}/\text{HD}/\text{gr}$ where an even larger width ($w = 0.16\text{--}0.25$) has been reported in Refs. 18, 19, simultaneous compression is impossible by adding only ^3He atoms.
- [34] A. F. Andreev, edited by D. F. Brewer, Progress in Low Temp. Phys., Vol. VIII (North-Holland, Amsterdam, 1982) pp. 67–131.
- [35] J. M. Kosterlitz and D. J. Thouless, J. Phys. C: Solid St. Phys. **6**, 1181 (1973); D. R. Nelson and J. M. Kosterlitz, Phys. Rev. Lett. **39**, 1201 (1977).